OPTO/MECHANICAL ANALYSIS FOR THE SPACE INTERFEROMETRY PROJECT GAIA

M. Cecconi[1], **G. Rigoni**[2], **P.L. Bernacca**[3]

[1]Ph.D. Course in Space Sciences and Technologies, Department of Astronomy, University of Padova, Italy
[2]Physics Course, Department of Physics, University of Padova, Italy
[3]Department of Astronomy and Space Center CISAS 'G.Colombo', University of Padova, Italy

ABSTRACT

The baseline optical configuration proposed by Perryman & Lindegren for the Global Astrometric Interferometer for Astrophysics (GAIA), was optically analysed and presented by Loiseau & Shacklan at the Cambridge Workshop on such a project. Since this configuration can be used in the case of a modulating grid for image location on the focal plane, we have improved it by optimizing with the ray-tracer CODE V only the edges instead of the full entrance pupil. We have obtained higher values for the visibilities of the fringes over the entire field of view ($\approx 0.45°$ radius). The field distorsion of the improved optical configuration is marginally larger but it can be calibrated. Other optical quality parameters such as spot diameters, Strehl ratio, optical path differences and visibilities are presented. An opto/mechanical analysis is also performed for this improved configuration to set tolerances of the optics. Such an analysis includes tilts around the three axis, decenters and pistons of all the mirrors of the interferometer and their figuring.

Key words: space interferometry; GAIA, optical design.

1. INTRODUCTION

The Global Astrometric Interferometer for Astrophysics (GAIA) has been proposed by Lindegren & Perryman (1994) for high precision astrometric measurements on about 50 millions of stars, following the success of the Hipparcos mission. An optical configuration for GAIA has been analysed by Loiseau & Shaklan (1995, 1996). Starting from such a configuration, we have found another one, Rigoni (1996) and Cecconi (1996), similar in the concept and improving the outcomes, saving the ≈ 11.5m effective focal length, the apertures diameter and their interdistance. Opto/mechanical analysis has been performed to study the tolerances (figuring and positioning) of the optical surfaces Shaklan & Loiseau 1996.

2. OPTIMIZATION OF THE OPTICAL CONFIGURATION

The optical configuration for GAIA proposed by Loiseau & Shaklan fits the mission requirements, but slightly different optical parameters allow a better performance of the instrument.

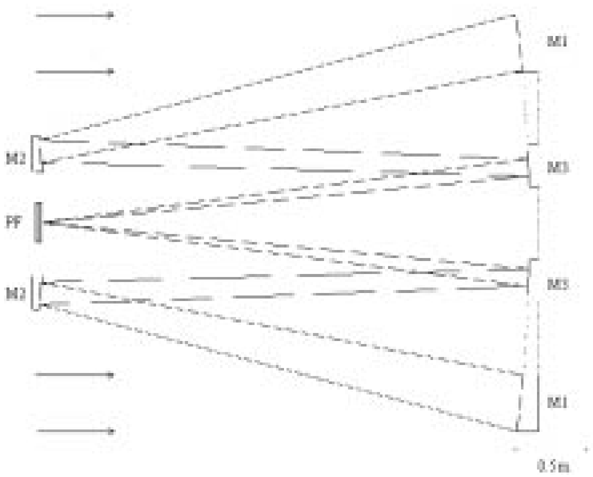

Figure 1. Layout of the GAIA interferometer. The primary and the secondary surface have the same vertex, while the focal plane is near the secondary mirrors.

The parameters here presented were obtained as result of an optimization process implemented by the ray-tracer CODE V. Two expedients, both methodologically correct, made this possible:

1. the use of an entrance pupil whose shape is the smallest ring that contains both the interferometer apertures (see Figure 2). This allows to neglect the central part of the mirrors, that is not used in the interferometer;
2. the definition of an error function that comprises terms based on the wavefront variance, beside the spot diagrams size. In this way the wave nature of the light is considered, as its effects are important in a diffraction-limited instrument.

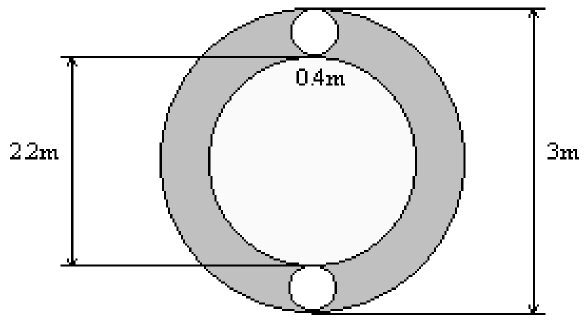

Figure 2. The entrance pupil of the interferometer (white circles) and the EP which have been used in the optimization process (gray ring).

The resulting optical parameters are shown in Table 1 while Table 2 shows the optical quality parameters by which the improved performances have been verified.

Table 1. Optical parameters obtained after the optimization process. z is the vertex coordinate, R is the radius of curvature and K is the conic constant.

Surface	z (mm)	R (mm)	K
Primary mirror	3520.000	-11503.850	-1.396601
Secondary mirror	20.000	-5258.058	-3.474096
Tertiary mirror	3520.000	-9894.692	-4.859013
Focal plane	-0.009975	∞	-

In the new configuration the full aperture spot sizes are a bit larger than those of the previous configuration but the interferometric ones are smaller. This gives a first information about the improvement obtained for the interferometer. The new configuration presents a slightly larger field distortion, that is quantitatively given by the shift of the Point Spread Function (PSF) centroid from the chief ray, or Gaussian image, but it can be calibrated. Other parameters such as the wavefront variance and the Strehl ratio emphasize that the instrument is diffraction limited. The separation of the centroids of the Airy disks associated to the two single apertures of the interferometer, are reduced by a factor of 1/2, and the fringe visibility has the ideal value of 1.000 (at 550 nm). Y-direction seems to be more critical.

3. OPTO/MECHANICAL ANALYSIS OF THE OPTICAL CONFIGURATION

The nominal optical configuration represented by the parameters of Table 1 is only ideal because the optical surfaces can change in shape and position for different causes. So, small perturbations have been applied to optical surfaces to analyse the monochromatic on-axis PSF behaviour.

Table 2. The main optical quality parameters for the new configuration are shown for five directions in the field of view: (a) interferometric (μm); (b) OPD RMS (λ/1000); (c) Strehl; (d) Field distortion (μm); (e) Centroid separation (μm); (f) Fringe visibility.

x-angle	0.00°	0.00°	0.00°	0.32°	0.45°
y-angle	0.00°	0.32°	0.45°	0.00°	0.00°
(a)	1.04	3.12	4.20	1.09	1.29
(b)	2	12	17	3	5
(c)	1.000	0.994	0.989	1.000	0.999
(d)	0.00	0.00	0.00	-2.11	-3.05
	0.00	-2.12	-3.45	0.00	0.00
(e)	0.50	0.11	0.06	0.76	1.04
(f)	1.000	1.000	1.000	1.000	1.000

3.1. Changes in Shape of Optical Surfaces

The nominal shape of the optical surfaces can change during their manufacturing and/or in-flight, after their integration in the satellite, because of stresses during launch and thermal and gravity gradients. The shape of the optical surfaces included in the examined configuration is determined by radius of curvature R and conical constant K. To simulate the manufacturing defects, the nominal values of R and K have been independently perturbed at first for only one aperture (a) and then for both apertures (b). In Table 3 the corresponding tolerances acceptable to satisfy coherence condition (appearance of fringes) of the interferometer are reported.

Table 3. Acceptable tolerances for cases (a) and (b) for shape changes caused by defects in the manufacturing of the optical surfaces.

	ΔR (μm)		ΔK ($\times 10^{-4}$)	
	(a)	(b)	(a)	(b)
M1	50 ÷ 80	10 ÷830	5 ÷810	1 ÷ 5
M2	50 ÷ 100	10 ÷ 40	10 ÷ 40	10 ÷ 30
M3	100 ÷ 500	10 ÷ 50	40 ÷ 80	10 ÷ 40

To simulate the in-flight changes of shape, the nominal values of R and K have been independently perturbed at first for only one aperture (a) and then for both apertures (b) but the mirrors have been recentered on their nominal position. In Table 4 the corresponding tolerances acceptable to satisfy coherence condition are reported.

3.2. Changes in Position of Optical Surfaces

Perturbations of the nominal positions of the optical surfaces also cause variations on the resulting point spread functions. Tilts around the three reference axis, decenters normally to the optical axes and pistons have been considered to obtain the acceptable mechanical tolerances.

Table 4. Acceptable tolerances for cases (a) and (b) for in-flight changes of shape of the optical surfaces.

	ΔR (mm)		ΔK ($\times 10^{-4}$)	
	(a)	(b)	(a)	(b)
M1	< 1.1	< 0.6	< 7	< 1
M2	< 2.6	< 1.1	< 17	< 10
M3	< 9.9	< 4.9	< 340	< 146

3.2.1. Tilts

We have tilted the optical surfaces around axis in three ways sketched in Figure 3 for α-tilts. In Table 5 the corresponding tollerances are reported.

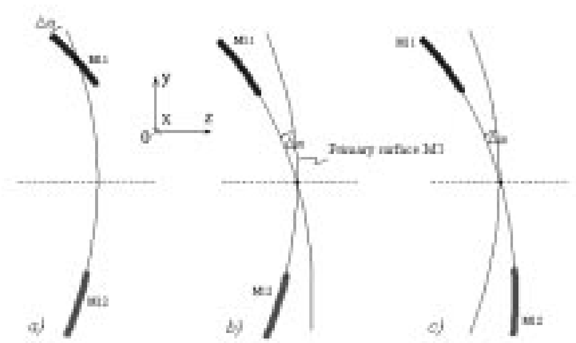

Figure 3. Tilts of the optical surfaces. Only the α-tilt is sketched in the figure. The other ones are analogous. Types (a) and (b) produce about the same perturbation in the PSFs for α- and β-tilts. γ-tilt is important only in the type (a) because the other two types should cause a changing in orientation and number of fringes. Types (a) and (b) cause a separation of the Airy disks while type (c) causes only a displacement of the PSFs from their original position. For type (c), the tolerances have been searched for saving such position.

3.2.2. Decenters

We have decentered the optical surfaces along two directions normally to the optical axis, along baseline (y-direction) and normally to it (x-direction). In Table 6 the corresponding tollerances are reported.

3.2.3. Pistons

We have pistoned the optical surfaces, that is, they have been moved along the direction z of the optical axis. In Table 7 the corresponding tolerances are reported.

Table 5. Acceptable tolerances for cases (a) and (c) for tilts of the optical surfaces.

	$\Delta\alpha$ (mas)		$\Delta\beta$ (mas)		$\Delta\gamma$ (arcsec)
	(a)	(c)	(a)	(c)	(a)
M1	< 100	< 50	< 100	< 50	< 1
M2	< 200	< 100	< 200	< 100	< 2
M3	< 300	< 200	< 300	< 200	< 10

Table 6. Acceptable tolerances for cases (a) and (b) for decenters of the optical surfaces.

	Δx (μm)		Δy (μm)	
	(a)	(b)	(a)	(b)
M1	< 8	< 1	< 8	< 1
M2	< 8	< 1	< 9	< 1
M3	< 20	< 2	< 20	< 2

4. CONCLUSIONS

The optical configuration we have analysed gives fringes with better contrast in comparison to the previous ones allowing to reach fainter magnitudes and larger astrometric precisions. By the opto/mechanical study of such a configuration, we have found the acceptable tolerances of the optical parameters to save the coherence condition of the interferometer. Manufacturing tolerances are more critical for the primary mirrors and less for the tertiary ones. Besides, defects on two mirrors of the same type are more critical than on only one. Tilts are more critical for the primary mirrors and less for the tertiary ones. An important result of such analysis is that a tilt of only one mirror splits the PSFs in the two Airy disks corresponding to the apertures while tilts of both the mirrors, with the optical surface generating them, causes only a shift of the PSFs. This result suggests to connect together the mirrors of the same type into a monolithical rigid mechanical structure. The decenters are more critical for primary and secondary mirrors than for tertiary ones. As it happens in the case of tilts, the decenters of only one mirror are more critical than those of both the mirrors of the same type because they cause a split of the PSFs in the two Airy disks instead of a simple shift of the fringes centroid. A rigid structure

Table 7. Acceptable tolerances for cases (a) and (b) for pistons of the optical surfaces.

	Δz (μm)	
	(a)	(b)
M1	< 30	< 20
M2	< 30	< 20
M3	< 150	< 80

is also suggested by such a result. The pistons are more critical for primary and secondary mirrors than for tertiary ones. In such a case, also the piston of two mirrors of the same type in the same direction, as they belong to the same rigid structure, causes a split of the PSFs in the two Airy disks (defocus). Such a qualitative opto/mechanical analysis could probably be applied on new optical configurations based on the same design as the one we have recently found (four mirrors, four reflections, $f = 25$ m).

REFERENCES

Cecconi, M., 1996, Opto/mechanical analysis for a space interferometry project (GAIA) in study under ESA, Space Sciences and Technologies Ph.D. Thesis, University of Padova, Italy

Lindegren, L., Perryman, M.A.C., 1994, A Concept for an ESA Cornerstone Mission, Supplementary Information submitted to the Horizon 2000+ Survey Committee

Loiseau, S., Shaklan, S., 1995, Analysis of an astrometric Fizeau interferometer for GAIA, ESA SP–379 Future possibilities for astrometry in Space, RGO-ESA Workshop, Cambridge, UK, 19-21 June 1995

Loiseau, S., Shaklan, S., 1996, Optical design, modelling and tolerancing of a Fizeau interferometer dedicated to astrometry, A&A Suppl., 117, 167

Rigoni, G., 1996, Optical analysis of the ESA space interferometer GAIA and simulated observations of double stars, Thesis in Physics, University of Padova, Italy